Arsenic trioxide enhances the therapeutic efficacy of radiation treatment of oral squamous carcinoma while protecting bone

Pawan Kumar, Qinghong Gao, Yu Ning, Zhuo Wang, Paul H. Krebsbach, and Peter J. Polverini

Department of Biologic and Materials Sciences, University of Michigan School of Dentistry, Ann Arbor, Michigan

Abstract

Therapeutic radiation is commonly used in the treatment of squamous cell carcinoma of the oral cavity and pharynx. Despite the proven efficacy of this form of anticancer therapy, high-dose radiation treatment is invariably associated with numerous unwanted side effects. This is particularly true for bone, in which radiation treatment often leads to osteoradionecrosis. The aim of this study was to investigate if treatment with arsenic trioxide (As_2O_3) could enhance the antitumor effect of radiotherapy whereas minimizing the destructive effects of radiation on bone. As_2O_3 treatment induced a dose-dependent (1 – 20 μmol/L) inhibition of endothelial and tumor cell (OSCC-3 and UM-SCC-74A) survival and significantly enhanced radiation-induced endothelial cell and tumor cell death. In contrast, As_2O_3 treatment (0.5 – 7.5 μmol/L) induced the proliferation of osteoblasts and also protected osteoblasts against radiation-induced cell death. Furthermore, As_2O_3 treatment was able to significantly enhance radiation-induced inhibition of endothelial cell tube formation and tumor cell colony formation. To test the effectiveness of As_2O_3 and radiation treatment *in vivo*, we used a severe combined immunodeficiency mouse model that has a bone ossicle and tumor growing side by side subcutaneously. Animals treated with As_2O_3 and radiation showed a significant inhibition of tumor growth, tumor angiogenesis, and tumor metastasis to the lungs as compared with As_2O_3 treatment or radiation treatment alone. In contrast, As_2O_3 treatment protected bone ossicles from radiation-induced bone loss. These results suggest a novel strategy to enhance the therapeutic efficacy of radiation treatment while protecting bone from the adverse effects of therapeutic radiation. [Mol Cancer Ther 2008;7(7):2060 – 9]

Received 8/29/07; revised 3/24/08; accepted 5/20/08.

Grant support: University of Michigan's Head and Neck Cancer Specialized Programs of Research Excellence grant 5 P50 CA097248 (P. Kumar).

The costs of publication of this article were defrayed in part by the payment of page charges. This article must therefore be hereby marked *advertisement* in accordance with 18 U.S.C. Section 1734 solely to indicate this fact.

Note: Present address Q. Gao: Department of Oral and Maxillofacial Surgery, SiChuan University, ChengDu, Sichuan, China.

Requests for reprints: Pawan Kumar, Department of Biologic and Materials Sciences, University of Michigan School of Dentistry, 1011 North University Avenue, Room no. 5205, Ann Arbor, MI 48109. Phone: 734-647-7599; Fax: 734-647-2110. E-mail: pksuri@umich.edu or Peter J. Polverini, University of Michigan School of Dentistry, 1011 North University Avenue, Room no. 1234, Ann Arbor, MI 48109. Phone: 734-763-3311; Fax: 734-763-5142. E-mail: neovas@umich.edu

doi:10.1158/1535-7163.MCT-08-0287

Introduction

Squamous cell carcinoma of the oral cavity and pharynx is a major worldwide health care problem (1). Many of these cancer patients receive high-dose radiotherapy encompassing large areas of the oral cavity, maxilla, and mandible. Despite having the advantage of preserving the tissue structure, high-dose radiotherapy causes considerable collateral damage to normal cell populations at the treatment site (2). This is particularly true for bone, in which radiation treatment often leads to bone destruction and impaired healing (3). Osteoblasts exposed to ionizing radiation exhibit decreased collagen synthesis and lead to bone atrophy and osteonecrosis (4–6). Because radiotherapy-induced osteoradionecrosis causes high morbidity and leads to a reduced quality of life, the aim of this study was to explore novel strategies to enhance the therapeutic efficacy of radiotherapy while protecting the surrounding bone.

Arsenicals have been used for centuries to treat a variety of medical conditions including cancers. Arsenic trioxide (As_2O_3) is currently Food and Drug Administration–approved and has been successfully used to treat patients with acute promyelocytic leukemia. As_2O_3 treatment has shown remarkable clinical responses in patients with acute promyelocytic leukemia (7), by causing both tumor cell differentiation at low concentrations (0.1–0.5 μmol/L) and by inducing apoptosis at relatively high concentrations (>0.5 μmol/L, ref. 8). Because the latter effect is not specific to acute promyelocytic leukemia, a number of preclinical studies and clinical trials are ongoing to evaluate its efficacy for treating a variety of solid tumors (9, 10). Similar to tumor cells, As_2O_3 treatment is equally effective in inducing endothelial cell apoptosis and inhibiting angiogenesis (11). The precise mechanisms by which As_2O_3 mediates its effects are not well understood. Some studies have indicated that As_2O_3 down-regulates the expression of Bcl-2 (12) and activates caspase-3–like caspase activity (13), whereas other studies have suggested that As_2O_3 induces apoptosis by a direct effect on the mitochondrial permeability and loss of mitochondrial transmembrane potential (14). Recently, the generation of reactive oxygen species has also been reported to regulate As_2O_3-induced apoptosis (13).

p38 mitogen-activated protein kinase (MAPK) plays an important role in cell survival or cell death depending on the cell type. We and others have previously shown that p38 MAPK is a key cell death pathway in endothelial cells and in a number of tumor cell types (15–17). In contrast, activation of p38 MAPK has been shown to mediate osteoblast proliferation and differentiation (18, 19). Thus, p38 MAPK provides us with a unique therapeutic target to inhibit tumor growth and tumor angiogenesis while at the same time having a protective effect on the surrounding bone tissue. However, no selective activator of p38 MAPK is currently available. As_2O_3 has been shown to activate p38 MAPK in a number of cell types (17, 20, 21). We selected As_2O_3 for this study because it has been successfully used in clinical protocols to treat patients with acute promyelocytic leukemia (7) and provides us the opportunity to examine if As_2O_3 treatment could enhance the therapeutic efficacy of radiotherapy while protecting the surrounding bone tissue. If this strategy works, it may prove to be very beneficial for head and neck cancer patients in which tumors undergoing radiation therapy are often present in close proximity to bone.

Although recent studies have shown the effectiveness of As_2O_3 treatment in inhibiting tumor growth and tumor angiogenesis, little information is available regarding the effects of As_2O_3 on osteoblasts and bone function. In this study, we investigated if treatment with As_2O_3 could enhance the antitumor and antiangiogenesis effects of radiation treatment while protecting bone from the negative effects of radiation. We report here that As_2O_3 treatment significantly enhances the therapeutic efficacy of radiation treatment by inhibiting tumor growth, tumor angiogenesis, and tumor metastasis whereas minimizing bone loss. This approach may provide a novel strategy to enhance the therapeutic efficacy of radiation treatment by enhancing the apoptosis of tumor cells and endothelial cells lining the tumor blood vessels while protecting bone from the adverse effects of therapeutic radiation.

Materials and Methods

Cell Cultures

Primary human dermal microvascular endothelial cells (HDMEC) and primary normal human osteoblasts (NHOst) were purchased from Bio Whittaker. HDMECs were maintained in endothelial cell basal medium-2 containing 5% fetal bovine serum and growth supplements. NHOst were maintained in osteoblast basal medium containing 10% FBS and growth supplements. Oral squamous carcinoma cells (OSCC-3) and UM-SCC-74A cells (a squamous carcinoma cell line derived from the base of the tongue) were maintained in DMEM supplemented with 10% FBS.

Survival Assay

Cell survival was assessed using a modified MTT assay. HDMEC, NHOst, and OSCC-3 cells were plated in flat-bottomed 96-well microtiter plates at a density of 5×10^3, 5×10^3, and 3×10^3 cells/well, respectively. After 24 h, cells were washed and treated with different concentrations of As_2O_3 (0.5–20 μmol/L; Sigma). For combination treatment, cells were treated with As_2O_3 for 1 h and then exposed to a single dose of γ-irradiation (7.5 Gy) and cultured for an additional 72 h. At the completion of incubation, cell survival was assessed by adding 10 μL of WST/ECS solution (BioVision) into each well and incubating at 37°C for 2 to 4 h (2 h for OSCC-3 and 4 h for HDMEC and NHOst). The reaction was stopped by adding 1% SDS and plates were read on a microplate reader (Sectramax M2; Molecular Devices, Corp.) at a wavelength of 440 nm. The percentage of survival for each group was calculated by adjusting the control group to 100%. Each test group was run in eight wells and each assay was repeated at least three times.

Apoptosis Assay

HDMEC, NHOst, and OSCC-3 cells were cultured in 6 cm dishes. After 24 h, cells were treated with As_2O_3 for 1 h and then exposed to a single dose of ionizing radiation (7.5 Gy) and cultured for an additional 72 h. At the completion of incubation, cells were retrieved, fixed in 4% paraformaldehyde for 15 min at 4°C, and then stored overnight in 70% ethanol at −20°C. The percentage of apoptotic cells was evaluated using the APO-BRDU terminal deoxynucleotidyl transferase–mediated dUTP-biotin nick end labeling (TUNEL) kit according to the manufacturer's instructions (Sigma). Apoptotic cells were quantified by flow cytometry using an argon laser excited at 488 nm (BD Biosciences).

Matrigel *In vitro* Endothelial Tube Formation Assay

Matrigel (125 μL, growth factor reduced), after thawing on ice, was plated in eight-well chamber slides (22). These slides were then incubated at 37°C for 30 min to allow the Matrigel to polymerize. HDMECs (400 μL; 4×10^4 cells/mL in endothelial cell basal medium-2 supplemented with 2% serum) were added to each well and treated with vascular endothelial growth factor (VEGF; 50 ng/mL) in the presence or absence of As_2O_3. The chamber slides were then incubated for 16 to 18 h at 37°C in 5% CO_2 humidified atmosphere. At the end of the incubation period, the culture medium was very carefully aspirated off the Matrigel surface and the cells were fixed with methanol and stained with Diff-Quick solution II. Each chamber was photographed (LEICA DM-IRB microscope and LEICA DC500 camera) at ×50 magnification and the total area occupied by the endothelial cell–derived tubes in each chamber was calculated using Metamorph software (Universal Imaging Corporation) and expressed as an angiogenic score.

Tumor Cell Colony Formation Assay

Colony formation assay was done in a 24-well culture plate. Three hundred microliters of a base layer of 0.6% (w/v) agarose (Ultra Pure, Invitrogen) was prepared by mixing autoclaved 1.2% (w/v) agarose solution with 2× DMEM supplemented with 20% FBS in a 1:1 ratio. The tumor cell (OSCC-3 or UM-SCC-74A) suspension was prepared by trypsin/EDTA treatment and a working cell suspension containing 2.5×10^4 cells/mL was prepared in a 1:1 mixture of 1.2% (w/v) agarose (Low Melting

Point, Invitrogen) solution and 2× DMEM supplemented with 20% FBS. Four hundred microliters of the cell suspension was carefully layered on top of the base layer. The plates were sealed and incubated at 4°C to allow the agarose to solidify. After 30 min, plates were transferred to 37°C and incubated overnight. The next day, 400 μL of 2× As_2O_3 in medium was added to the appropriate wells. After 14 days of culture, the number of colonies was counted and photographed using LEICA DM-IRB microscope equipped with LEICA DC500 camera at ×50 magnification.

In vivo Tumor Development and Bone Formation Assay

To test the effectiveness of As_2O_3 and radiation treatment *in vivo*, we developed a severe combined immunodeficiency (SCID) mouse model that has a bone ossicle and tumor growing side by side.

Isolation and Culture of Bone Marrow Stromal Cells. The femur, tibia, and humerus of donor animals (8-week-old BALB/c mice; Charles River) were excised and adherent tissue was dissected. The marrow from these bones was collected by flushing with HBSS (Life Technologies) using a 5 mL syringe fitted with a 23-gauge needle (23). A single cell suspension was prepared by gently passing them through a syringe. Cells were then passed through a cell strainer to remove the debris and cellular aggregates. Bone marrow cells were washed twice with HBSS and cultured in α-modified Eagle's medium (Life Technologies) supplemented with 10% FBS. Once the bone marrow stromal cells (BMSC) reached ~80% to 90% confluency, they were transduced with BMP-2 using adenovirus vector expressing BMP-2 (adCMVBMP-2; ref. 24).

Implantation of BMSCs, Tumor Cells, and Endothelial Cells (HDMEC). Gelfoam sponges were used to implant BMSCs into the flanks of SCID mice (25). In brief, 3 × 3 mm^2 gelfoam sponges were prepared and washed with α-modified Eagle's medium. BMSCs (2 × 10^6) transduced with BMP-2 were incorporated into each sponge. One sponge was implanted into the flanks of each SCID mouse. After 2 weeks, once the palpable bone ossicles were formed, tumor cells (OSCC-3 or UMSCC-74A, 0.5 × 10^6 cells) and HDMECs (0.5 × 10^6 cells) were mixed with 100 μL of Matrigel and the cell mixture was implanted into the flanks of SCID mice adjacent to the bone ossicles. Tumors were allowed to grow and vascularize for 8 days and then treated with As_2O_3 (2, 5, and 10 mg/kg on days 8, 12, and 15, respectively) and three fractionated doses of ionizing radiation (7.5 Gy × 3, on days 9, 13, and 16). Tumor volume measurements began on day 1 (tumor inoculation) and continued twice a week until the end of the study. Tumor volumes were calculated using the formula, volume (mm^3) = $L \times W^2 / 2$ (length, L; width, W; in millimeters). Length and width were measured using a digital caliper. One week after the last treatment (day 23), tumors and lungs were removed and analyzed for tumor growth, tumor angiogenesis, and tumor metastasis to lungs; bone ossicles were analyzed for bone mineral density.

Analysis of Bone Ossicles by Microcomputed Tomography

Bone ossicles retrieved from the tumor site were fixed in aqueous buffered zinc formalin (Anatech, Ltd.) for 24 h at 4°C. For microcomputed tomography analysis, bone ossicles were scanned at 8.93 μm voxel resolution (EVS, Corp.) for a total of 667 slices per scan. GEMS Micro View software was used to make a three-dimensional reconstruction from the set of scans. A fixed threshold was used to extract the mineralized bone phase, actual bone volume, and bone mineral density was calculated.

Analysis of Tumor Metastasis to Lungs

Lungs from SCID mice were carefully retrieved on day 23, fixed and paraffin embedded. Five-step sections of 5 μm with 100-μm spaces were cut and stained with H&E. The number of metastasis nodules present in these sections was counted using a Leica DM500 microscope at ×100 magnification.

Analysis of Tumor Angiogenesis by Immunolocalization of Von Willebrand Factor

Tissue sections were deparaffinized and antigen retrieval was achieved by pressure cooking in Decloaking chamber (Biocare Medical) at 120°C for 20 min (22). Tissue sections were then treated with a peroxide block solution for 5 min at room temperature followed by 1 h of incubation with primary antibody (anti–Von Willebrand factor; Dako) at room temperature. Slides were further incubated for 30 min with horseradish peroxidase–labeled polymer (Dako EnVision+ System Kit) and developed with AEC+ chromogen (Von Willebrand factor). Microvessel density in the tumor sections was calculated by counting six random fields (×200).

Statistical Analysis

Data from all the experiments were expressed as mean ± SE. Statistical differences were determined by two-way ANOVA and Student's t test. $P < 0.05$ was considered significant.

Results

As_2O_3 Induces a Dose-Dependent Inhibition of Endothelial and Tumor Cell Proliferation

Arsenic treatment of tumor cells (OSCC-3) resulted in a dose-dependent inhibition of OSCC-3 survival with 1%, 6%, 11%, 24%, 38%, 56%, and 67% inhibition at 0.5, 1, 2.5, 5, 7.5, 10, and 20 μmol/L, respectively (Fig. 1A). Similarly, As_2O_3 induced a dose-dependent inhibition of endothelial cell survival with 8%, 13%, 53%, 65%, and 76% inhibition at 2.5, 5, 7.5, 10, and 20 μmol/L, respectively (Fig. 1A). However, at low doses (0.5 and 1 μmol/L), As_2O_3 treatment of endothelial cells (HDMEC) resulted in a marginal increase (3% and 7%, respectively) in endothelial cell proliferation (Fig. 1A).

As_2O_3 Induces a Dose-Dependent Increase in Osteoblast Proliferation

In contrast to endothelial and tumor cells, osteoblasts (NHOst) treated with As_2O_3 showed the opposite effect. NHOst exposed to 0.5, 1, 2.5, 5, and 7.5 μmol/L of As_2O_3

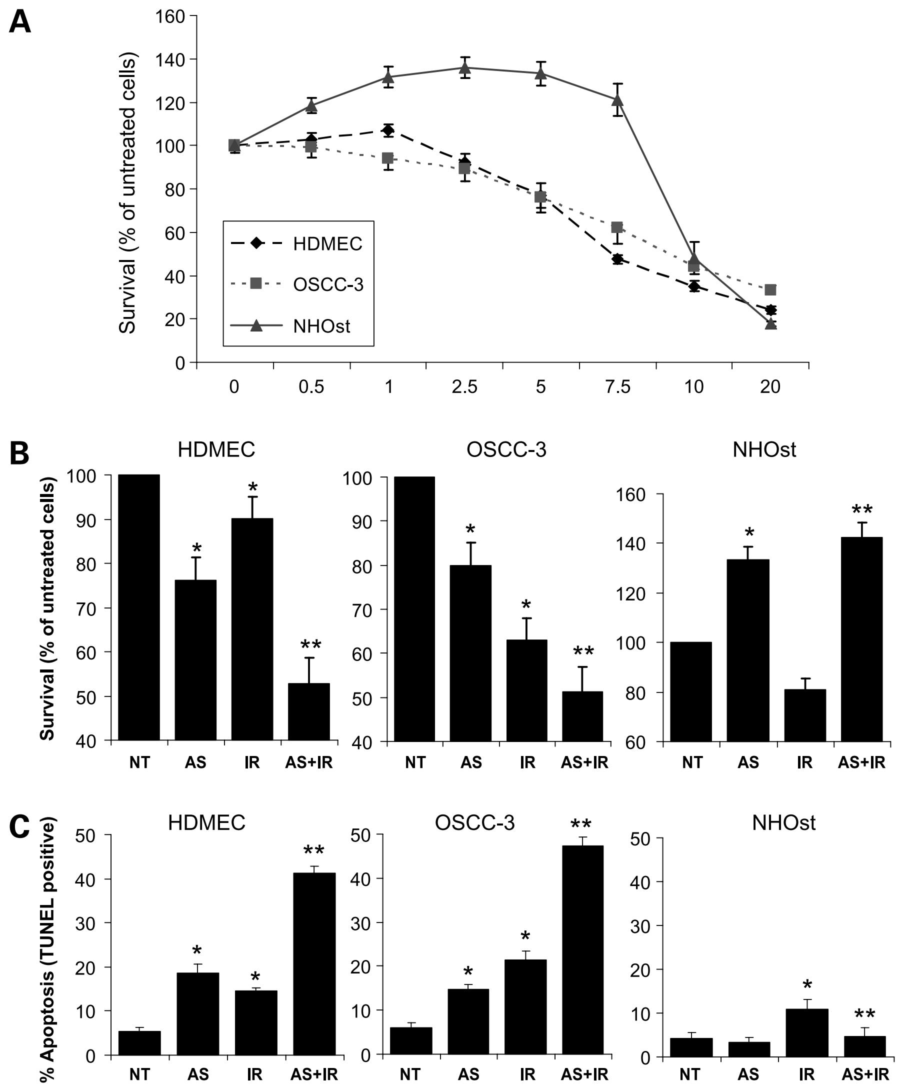

Figure 1. As_2O_3 enhances radiation-induced endothelial cell and tumor cell death while protecting osteoblasts. Endothelial cells (*HDMEC*, 5×10^3), tumor cells (*OSCC-3*, 3×10^3), and osteoblasts (*NHOst*, 5×10^3) were plated in 96-well plates at 37°C and cultured overnight. **A,** cells were treated with 0.5, 1, 2.5, 5, 10, and 20 μmol/L doses of As_2O_3. **B,** cells were treated with As_2O_3 (*AS*, 5 μmol/L) followed by radiation treatment (*IR*, 7.5 Gy). After 72 h of culture, 10 μL of WST/ECS solution (BioVision) was added into each well and these cells were further incubated at 37°C for 2 to 4 h (2 h for OSCC-3 and 4 h for HDMEC and NHOst). The reaction was stopped by adding 1% SDS and plates were read on a microplate reader at a wavelength of 440 nm. The percentage of survival was calculated by adjusting the control group (no treatment, *NT*) to 100%. Each test group was run in eight wells and each assay was repeated at least thrice. *, $P < 0.05$, significant difference as compared with the control group. **C,** HDMEC, OSCC-3, and NHOst cells were cultured in 6 cm dishes. After 24 h, cells were treated with As_2O_3 (*AS*, 5 μmol/L) for 1 h and then exposed to a single dose of γ-irradiation (7.5 Gy) and cultured for an additional 72 h. Upon completion of incubation, cells were harvested and the percentage of apoptotic cells was evaluated by the TUNEL assay according to the manufacturer's instructions (Sigma). *, $P < 0.05$, significant difference as compared with the control group.

showed a dose-dependent increase in cell proliferation at 18%, 32%, 36%, 33%, and 21%, respectively (Fig. 1A). However, As_2O_3 at higher concentrations (10 and 20 μmol/L) inhibited NHOst proliferation.

As_2O_3 Enhances Radiation-Induced Endothelial and Tumor Cell Death

For combination treatment, cells were treated with As_2O_3 (5 μmol/L) for 1 h and then exposed to ionizing radiation (7.5 Gy). As_2O_3 treatment significantly enhanced radiation-induced HDMEC cell death (47%, MTT assay; Fig. 1B and 42%, TUNEL assay; Fig. 1C). This was significantly higher than As_2O_3 treatment alone (24%, MTT assay; Fig. 1B and 18%, TUNEL assay; Fig. 1C) or radiation treatment (10%, MTT assay; Fig. 1B and 15%, TUNEL assay; Fig. 1C). Similarly, combination treatment with As_2O_3 and radiation induced a marked increase in OSCC-3 cell death (49%, MTT assay; Fig. 1B and 48%, TUNEL assay; Fig. 1C) as compared with As_2O_3 (20%, MTT assay; Fig. 1B and 16%, TUNEL assay; Fig. 1C) or radiation treatment alone (42%, MTT assay; Fig. 1B and 22%, TUNEL assay; Fig. 1C).

As_2O_3 Protects Osteoblasts from Ionizing Radiation–Induced Cell Death

In contrast with HDMEC and OSCC-3, As_2O_3 treatment significantly protected NHOst from radiation-induced cell death. When treated with radiation alone, NHOst cells showed a 15% decrease in survival (Fig. 1B). However, As_2O_3 treatment of NHOst prior to ionizing radiation exposure not only inhibited radiation-induced cell death, but also significantly increased NHOst proliferation (40%; Fig. 1B and C).

As_2O_3 Inhibits VEGF-Mediated Endothelial Cell Tube Formation

We evaluated the effect of As_2O_3 on angiogenesis using an *in vitro* endothelial cell tube formation assay. VEGF treatment of HDMEC significantly enhanced tube formation on growth factor–reduced Matrigel (Fig. 2). As_2O_3 treatment inhibited VEGF-mediated HDMEC tube formation in a dose-dependent manner with an 8%, 28%, 57%, and 100% inhibition at 2.5, 5, 10, and 20 μmol/L As_2O_3 dose, respectively (Fig. 2A and B). In addition, As_2O_3 treatment (5 μmol/L) along with radiation treatment (7.5 Gy) completely inhibited VEGF-mediated tube formation (Fig. 2C), whereas As_2O_3 treatment (5 μmol/L) alone or radiation treatment alone (7.5 Gy) showed 32% and 29% inhibition of endothelial cell tube formation (Fig. 2C).

As_2O_3 Inhibits Tumor Cell Colony Formation

We next investigated the effect of As_2O_3 on tumor cell colony formation. Tumor cells (OSCC-3 or UM-SCC-74A) were cultured in low–melting point agarose and treated with different concentrations of As_2O_3 for 14 days. As_2O_3 treatment induced a significant inhibition of tumor cell colony formation in a dose-dependent manner in both the tumor cell lines tested (data shown for OSCC-3; Fig. 3A and B). Similar to tube formation assay, As_2O_3 treatment (5 μmol/L) along with radiation treatment (7.5 Gy) induced a >90% inhibition of tumor cell colonies in both cell lines (Fig. 3C and D), whereas As_2O_3 treatment (5 μmol/L) alone or radiation treatment alone (7.5 Gy) showed 55% and 48% inhibition of OSCC-3 colonies, and 56% and 40% inhibition of UM-SCC-74A colonies, respectively (Fig. 3C and D).

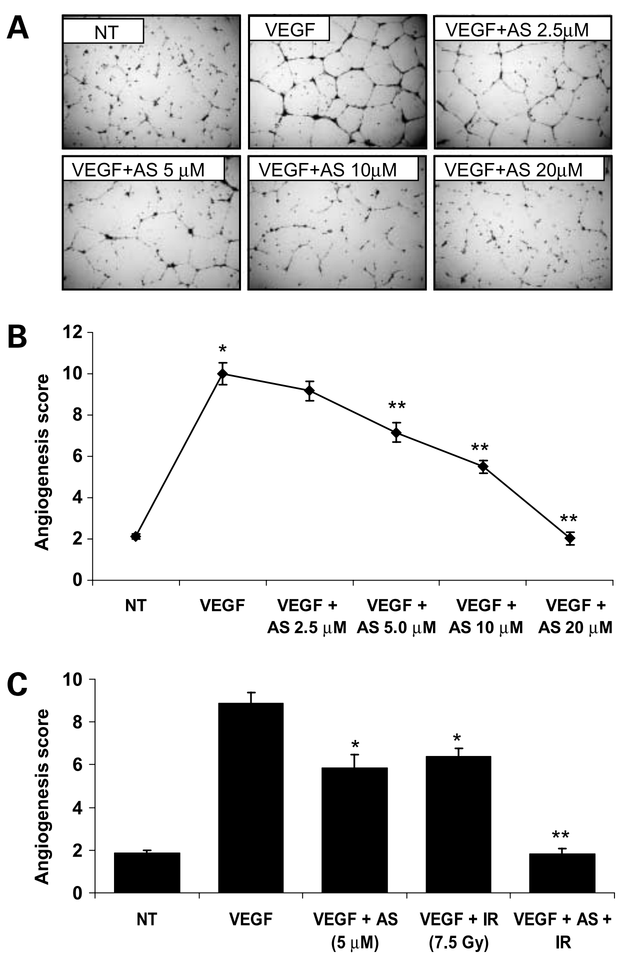

Figure 2. As_2O_3 enhances radiation-induced inhibition of endothelial cell tube formation. The Matrigel *in vitro* HDMEC tube formation assay was done in eight-well chamber slides. **A** and **B,** endothelial cells cultured on top of Matrigel were treated with VEGF and different doses of As_2O_3 (*AS*). **A,** photomicrographs of representative assays for no-treatment (*NT*), VEGF, VEGF + As_2O_3 (*AS*) 2.5 μmol/L, VEGF + AS 5 μmol/L, VEGF + AS 10 μmol/L, and VEGF + AS 20 μmol/L. **B,** quantitative data for HDMEC tube formation from three independent experiments (*points,* mean; *bars,* SE). **C,** HDMECs were cultured on top of Matrigel and were treated with VEGF alone or with radiation (7.5 Gy) and/or As_2O_3. *, $P < 0.05$, significant increase as compared with the no-treatment (*NT*) group; **, $P < 0.05$, significant decrease as compared with the VEGF group.

As_2O_3 and Radiation Treatment Significantly Inhibit Tumor Growth, Tumor Angiogenesis, and Tumor Metastasis

To corroborate our *in vitro* findings, we used a SCID mouse model to study the effects of As_2O_3 and radiation on tumor growth and bone (Fig. 4A). In this model, Gelfoam sponges seeded with BMSCs were implanted in the flanks of SCID mice to form bone ossicles (Fig. 4A). After 2 weeks, OSCC-3 cells and HDMEC were implanted adjacent to the mature bone ossicles. Animals were then treated with As_2O_3 (2, 5, and 10 mg/kg) and ionizing radiation. We observed severe systemic toxicity in animals receiving the 10 mg/kg As_2O_3 dose, therefore, we discontinued 10 mg/kg As_2O_3 treatment groups. Animals treated with As_2O_3 (5 mg/kg) and radiation together showed marked inhibition of tumor growth (39%, 49%, 54%, and 61% at days 12, 15, 18, and 21, respectively) which was highly significant as compared with the no-treatment group or animals treated with radiation alone (19%, 24%, 30%, and 38% at days 12, 15, 18, and 21, respectively) or As_2O_3 (2 mg/kg) treatment alone (12%, 14%, 17%, and 24% at days 12, 15, 18, and 21, respectively) or As_2O_3 (5 mg/kg) treatment alone (27%, 32%, 34%, and 42% at days 12, 15, 18, and 21, respectively) or As_2O_3 (2 mg/kg) and radiation combination treatment (32%, 35%, 37%, and 44% at days 12, 15, 18, and 21, respectively; Fig. 4C). In addition, tumor samples from As_2O_3 (5 mg/kg) and radiation treatment showed a marked increase in central tumor necrosis as compared with no treatment or single treatment alone (Fig. 4B). In order to further substantiate if the As_2O_3-mediated effect is not cell line–specific, we repeated this study using a second squamous cell line (UM-SCC-74A). As_2O_3 and radiation treatment showed marked inhibition of UM-SCC-74A tumors similar to that observed with OSCC-3 tumors (Fig. 4D).

We next analyzed the effects of As_2O_3 and radiation treatment on tumor angiogenesis by immunostaining paraffin-embedded tumor sections with anti-human Von Willebrand factor. As_2O_3 (5 mg/kg) and radiation treatment significantly inhibited tumor angiogenesis (65% for OSCC-3 tumors and 68% for UM-SCC-74A tumors; Fig. 5A and B) as compared with untreated controls. Animals treated with As_2O_3 alone showed 14% (2 mg/kg dose) and 35% (5 mg/kg dose) inhibition of tumor angiogenesis in OSCC-3 tumors, and 18% (2 mg/kg dose) and 32% (5 mg/kg dose) in UM-SCC-74A tumor, whereas animals given radiation treatment alone showed 23% and 30%

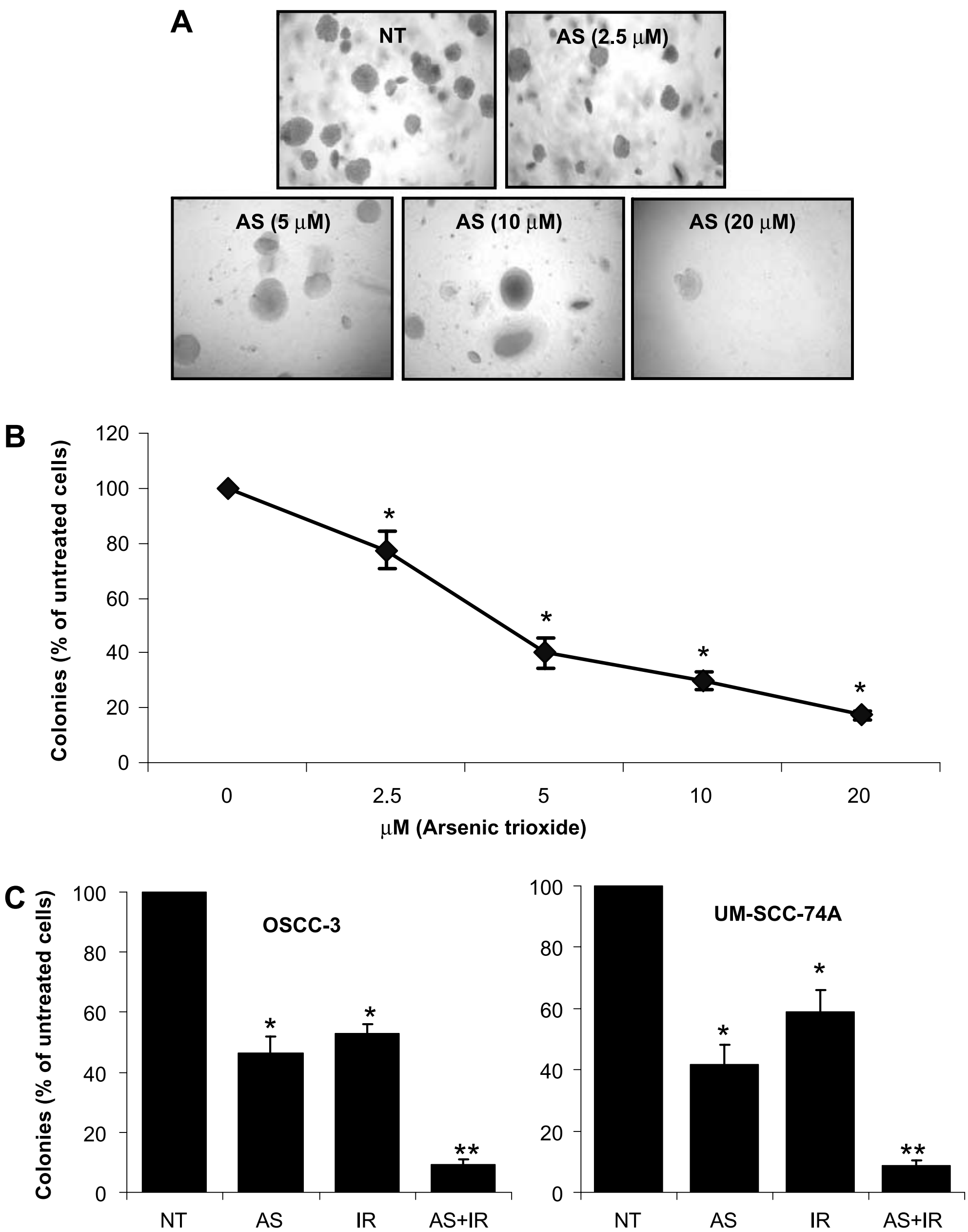

Figure 3. As_2O_3 enhances radiation-induced inhibition of tumor cell colony formation. The tumor cell colony formation assay was done in low-melting point agarose in 24-well plates. **A** and **B,** tumor cells (OSCC-3) were treated with different concentrations of As_2O_3 (2.5, 5, 10, and 20 μmol/L) and cultured for 14 d. **C** and **D,** tumor cells (OSCC-3 and UM-SCC-74A) were treated with As_2O_3 or radiation, or a combination of both and cultured for 14 d. The number of colonies formed in each test group was counted at low-power field (×50). The percentage of colonies formed was calculated by adjusting the control group (no treatment, *NT*) to 100%. *, $P < 0.05$, significant difference as compared with the no-treatment (*NT*) group; **, $P < 0.05$, significant difference as compared with As_2O_3 or radiation treatment alone.

tumor angiogenesis inhibition in OSCC-3 and UM-SCC-74A tumors, respectively. In addition, combination treatment with As_2O_3 and radiation significantly inhibited tumor metastasis to lungs (64% and 66% for OSCC-3 and UM-SCC-74A tumors, respectively) as compared with the no treatment group or As_2O_3 or radiation treatment alone group (Fig. 5C and D).

As_2O_3 Inhibits Radiation-Induced Bone Loss

The protective effect of As_2O_3 on radiation-induced bone loss was investigated by analyzing bone mineral density in bone ossicles. As_2O_3 treatment at 2 mg/kg and 5 mg/kg doses did not significantly affect bone mineral density in bone ossicles (Fig. 6A and B). But bone ossicles treated with three doses of ionizing radiation (7.5 Gy × 3) showed a significant decrease in bone mineral density as compared with the untreated group. As_2O_3 treatment at both 2 mg/kg and 5 mg/kg doses prior to each radiation treatment resulted in a significant reversal of radiation-induced bone loss (Fig. 6A and B).

Discussion

Radiotherapy is one of the most widely used treatments for oral and pharyngeal cancer. Although radiation treatment is often effective in inducing tumor regression, there are some serious drawbacks to its use, particularly in terms of its effects on normal bone growth and function (2). Osteoradionecrosis is perhaps the most serious clinical complication of radiation treatment in oral and pharyngeal cancer patients due to frequent juxtaposition of tumor and the jawbones during therapy (6). The development of new adjuvant therapies that enhance the therapeutic efficacy of radiation treatment whereas minimizing damage to normal tissue such as bone is of paramount importance for oral and pharyngeal cancer patients. In this study, we investigated whether treatment with As_2O_3, a known antitumor agent that activates both cell death and cell survival signaling pathway could enhance the therapeutic efficacy of radiation treatment while protecting the bone.

To test this hypothesis, we conducted experiments to examine the therapeutic efficacy and bone-protective effects of As_2O_3 and radiation for the treatment of oral squamous carcinoma, the most common form of oral and pharyngeal cancer. Our data showed that As_2O_3 induces a dose-dependent inhibition of tumor cell survival and colony formation. We also found that As_2O_3 induced a dose-dependent inhibition of endothelial cell survival and

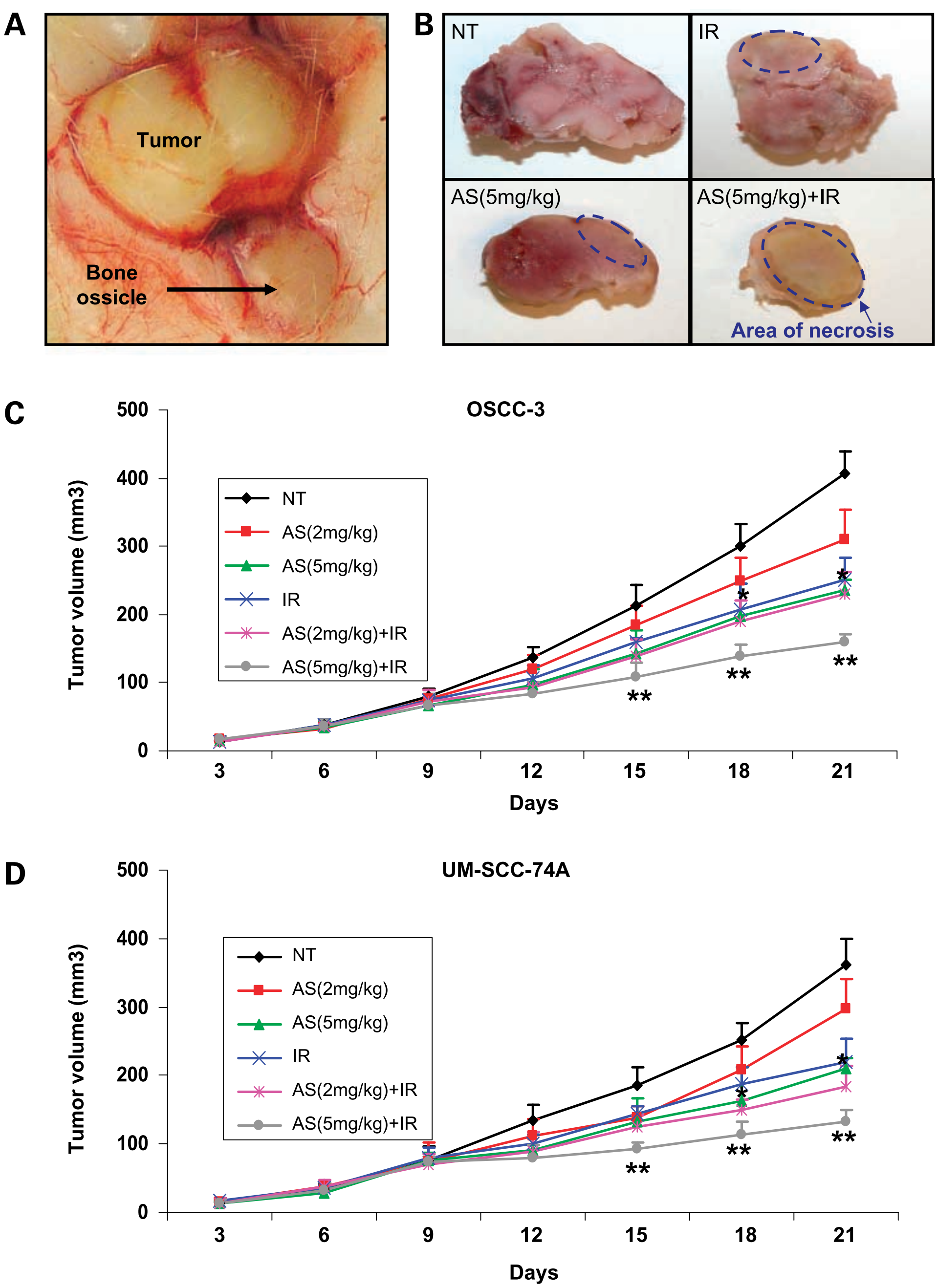

Figure 4. As_2O_3 and radiation treatment significantly inhibit tumor growth *in vivo*. Gelfoam carrier (3 × 3 mm^2) seeded with 2 × 10^6 BMSCs each were implanted into the flanks of 6-week-old SCID mice (eight animals/group). After 2 wk, tumor cells (OSCC-3 or UM-SCC-74A, 1 × 10^6) and HDMECs (1 × 10^6) were mixed with 100 μL of Matrigel and these cells were implanted into the flanks of SCID mice adjacent to the bone ossicles. Tumors were allowed to grow and vascularize for 8 d and then three doses of As_2O_3 (2 or 5 mg/kg, days 8, 12, and 15) and three fractionated doses of ionizing radiation (7.5 Gy × 3, days 9, 13, and 16) were administered. Tumor volume measurements began on day 1 (tumor inoculation) and continued twice a week until the end of the study. **A,** representative photomicrograph of tumor and bone ossicle growing side by side in a SCID mouse. **B,** cut tumors (OSCC-3) from no-treatment (*NT*), As_2O_3 5 mg/kg (*AS 5 mg/kg*), radiation treatment (*IR*), and As_2O_3 5 mg/kg + radiation treatment (*AS 5 mg/kg + IR*) groups. *Dotted circle* and *arrow,* areas of necrosis. **C** and **D,** tumor progression curves for OSCC-3 and UM-SCC-74A tumors treated with As_2O_3 (*AS*) or radiation treatment (*IR*) or As_2O_3 + radiation treatment (*AS + IR*). *, $P < 0.05$, significant difference as compared with the no-treatment group; **, $P < 0.05$, significant difference as compared with As_2O_3 or radiation treatment alone.

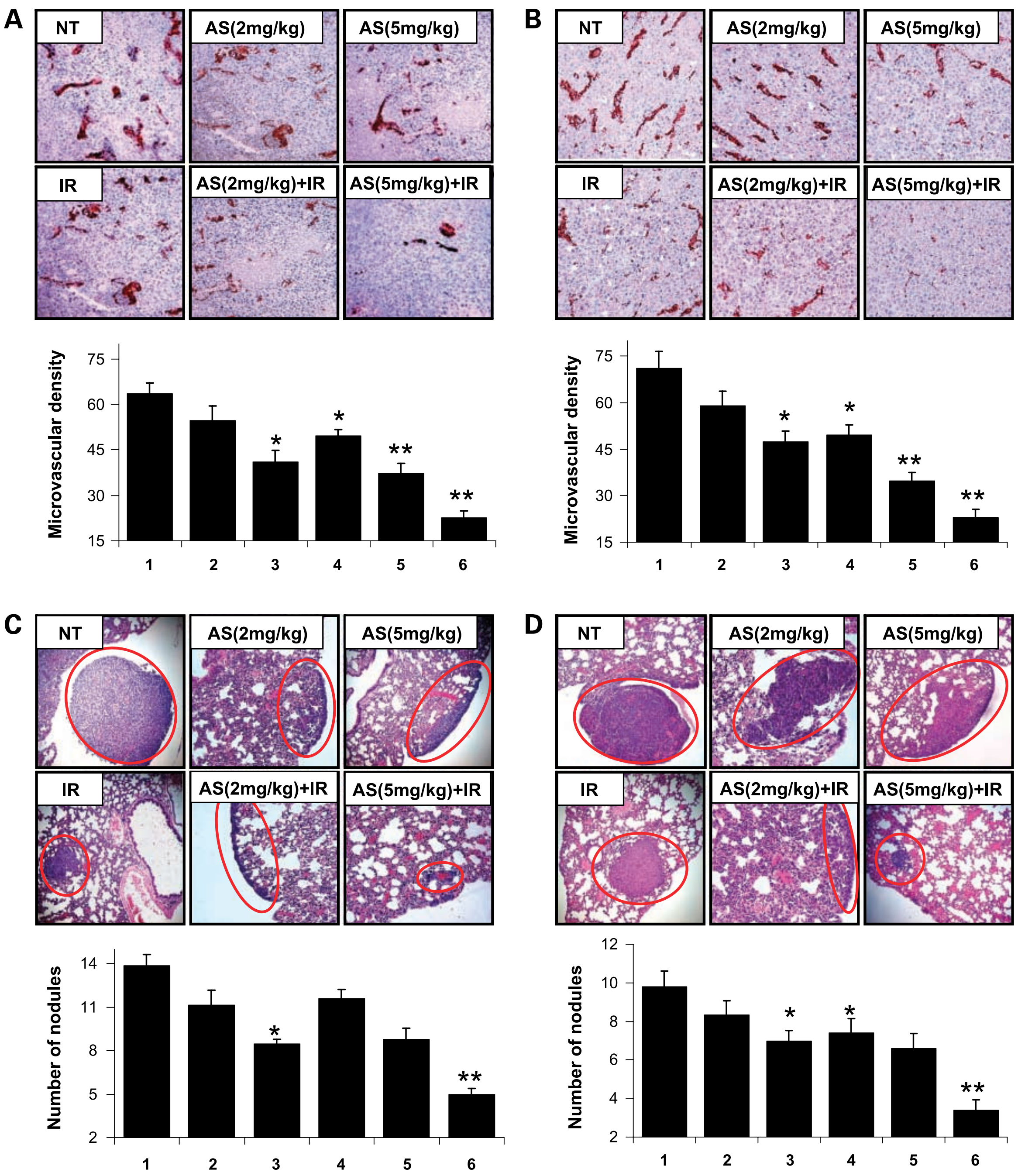

Figure 5. As_2O_3 and radiation treatment significantly inhibit tumor angiogenesis and tumor metastasis. **A** and **B,** paraffin-embedded tumor sections (OSCC-3, **A**; and UM-SCC-74A, **B**) were stained for tumor blood vessels using anti-human Von Willebrand factor antibodies. Representative photomicrographs of (*1*) no-treatment (*NT*), (*2*) As_2O_3 2 mg/kg (*AS 2 mg/kg*), (*3*) As_2O_3 5 mg/kg (*AS 5 mg/kg*), (*4*) radiation treatment (*IR*), (*5*) As_2O_3 2 mg/kg + radiation treatment (*AS 2 mg/kg + IR*), and (*6*) As_2O_3 5 mg/kg + radiation treatment (*AS 5 mg/kg + IR*). Microvessel density in the tumor samples was calculated by counting six random fields (×20). **C** and **D,** five paraffin-embedded (lungs) step sections of 5 μm with 100-μm spaces were cut and stained with H&E. The number of metastasis nodules present in these sections (OSCC-3, **C**; and UM-SCC-74A, **D**) was counted under the microscope. The treatment groups are the same as those described above (**A** and **B**). *, $P < 0.05$, significant difference as compared with the no-treatment group; **, $P < 0.05$, significant difference in AS + IR groups as compared with AS or IR alone.

tube formation on Matrigel. However, at very low doses (0.5 and 1 μmol/L), As_2O_3 potentiated endothelial cell proliferation. A number of studies (both *in vitro* as well as *in vivo*) have shown similar proangiogenic responses at low As_2O_3 treatment (26, 27). It is likely that low levels of As_2O_3 treatment preferentially induce the activation of proliferative pathways (28, 29). However, low doses of As_2O_3 most likely promote tumor angiogenesis by

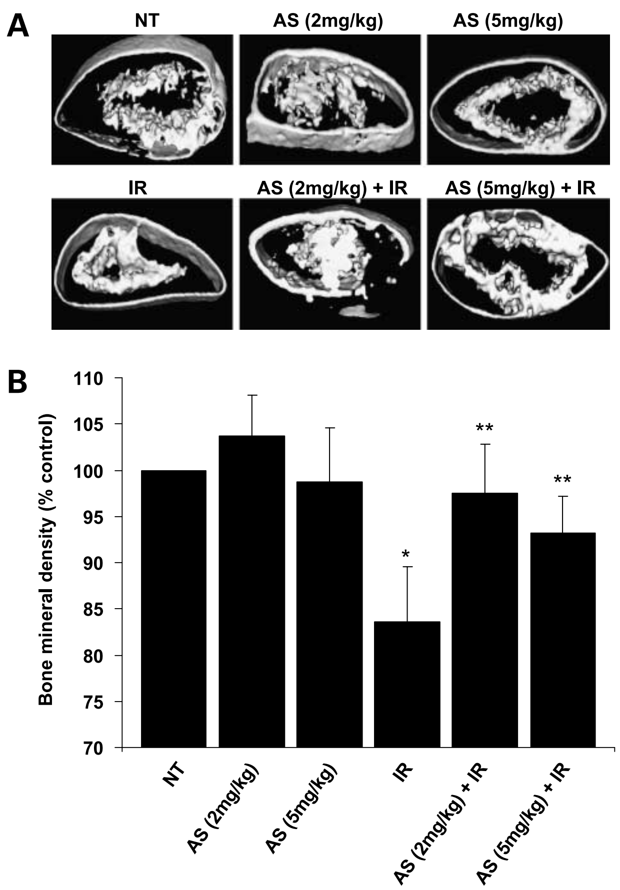

Figure 6. As_2O_3 treatment protects bone from radiation-induced bone loss. The bone ossicles were fixed in aqueous buffered zinc formalin and analyzed by microcomputed tomography for the bone mineral density. **A,** representative microcomputed tomography photomicrographs of no-treatment (*NT*), As_2O_3 2 mg/kg (*AS 2 mg/kg*), As_2O_3 5 mg/kg (*AS 5 mg/kg*), radiation treatment (*IR*), As_2O_3 2 mg/kg + radiation treatment (*AS 2 mg/kg + IR*), and As_2O_3 5 mg/kg + radiation treatment (*AS 5 mg/kg + IR*). **B,** bone mineral density data are expressed as mg/cc. *, $P < 0.05$, significant difference as compared with the no-treatment group; **, $P < 0.05$, significant difference in the AS + IR group as compared with IR alone.

stimulating the cells surrounding the endothelial cells in addition to its direct effect on endothelial cells (27).

In combination treatment studies, we selected a dose of 5 μmol/L of As_2O_3 because pharmacokinetic analysis of clinical samples has shown peak plasma arsenic concentrations to be ~5 μmol/L and the steady state is believed to be between 1 and 2 μmol/L (30). For radiation treatment, we selected 7.5 Gy dose that itself did not markedly induce endothelial cell or tumor cell death. Radiation treatment of tumor cells induced considerably more cell death as compared with endothelial cells at the same dose. As we have reported earlier, this is likely due to the fact that endothelial cells are normally quite resistant to radiation treatment due to their low turnover rate and elevated expression of the survival proteins Bcl-2 and survivin (31); consequently, tumor-associated endothelial cells require relatively high doses of radiation to induce significant endothelial cell death (22). The higher radiosensitivity of tumor cells could be due to their rapid rate of turnover, making the chromatin more susceptible to higher DNA damage caused by ionizing radiation. As_2O_3 treatment significantly enhanced radiation-induced endothelial cell as well as tumor cell death. In contrast, treatment of NHOst with As_2O_3 induced proliferation and protected osteoblasts against radiation-induced cell death. We speculate that this dichotomous response is likely due to the activation of p38 MAPK which has been shown to induce cell death in endothelial cells (15) and tumor cells (16, 17) while protecting osteoblasts and inducing osteoblast proliferation and differentiation (18, 19). Similarly, Hayashi et al. (32) have shown that As_2O_3 treatment was very effective in inducing apoptosis in multiple myeloma cells, whereas BMSCs (a precursor for bone cells) were highly resistant to As_2O_3 treatment even at very high doses (up to 100 μmol/L).

To confirm our *in vitro* studies and determine their pathophysiologic relevance, we developed a SCID mouse model in which tumor and bone were grown side by side. This mouse model allows us to study the effects of As_2O_3 and radiation treatment on tumor growth, tumor angiogenesis, and bone survival in an *in vivo* setting that mimics the clinical settings in oral and pharyngeal cancer patients in which tumors are often present in close proximity to bone. Similar to what we observed *in vitro*, As_2O_3 potentiated the antitumor and antiangiogenic effects of ionizing radiation, resulting in rapid and extensive tumor necrosis. As_2O_3 mediated inhibition of tumor growth could be due to its direct toxicity against tumor cells as well as its antiangiogenic activity. As_2O_3 is known to bind hemoglobin and can be distributed rapidly, especially to highly vascular tissues. Systemic treatment with As_2O_3 has been shown to induce a prompt and pronounced vascular shutdown in large murine tumors resulting in central tumor necrosis (33). The effect of As_2O_3 may also be more pronounced in the central tumor region due to its higher toxicity at regions of low pH and low pO_2 (34). The fact that As_2O_3 treatment has more pronounced effects against the central region and radiation treatment is normally more effective against the peripheral tumor area; therefore, this synergistic interaction between As_2O_3 and radiotherapy makes them an ideal combination treatment option.

In addition to enhancing the therapeutic efficacy of radiotherapy, As_2O_3 has an additional advantage of protecting bone tissue against radiation-induced bone loss. Therefore, this combination treatment strategy may be very beneficial to oral and pharyngeal cancer patients due to the presence of tumors often in close proximity to bone. Additional studies are planned to further investigate the role and molecular mechanism(s) by which As_2O_3 mediates bone protection.

Disclosure of Potential Conflicts of Interest

No potential conflicts of interest were disclosed.

Acknowledgments

We thank Dr. M. Lingen (University of Chicago) for the OSCC-3 cell line, Dr. T. Carey (University of Michigan) for the UM-SCC-74A cell line, and the Biological Resources Branch, National Cancer Institute, NIH, for the rhVEGF.

References

1. Dobrossy L. Epidemiology of head and neck cancer: magnitude of the problem. Cancer Metastasis Rev 2005;24:9 – 17.

2. Probert JC, Parker BR. The effects of radiation therapy on bone growth. Radiology 1975;114:155 – 62.

3. Green N, French S, Rodriquez G, Hays M, Fingerhut A. Radiation-induced delayed union of fractures. Radiology 1969;93:635 – 41.

4. Gal TJ, Munoz-Antonia T, Muro-Cacho CA, Klotch DW. Radiation effects on osteoblasts *in vitro*: a potential role in osteoradionecrosis. Arch Otolaryngol Head Neck Surg 2000;126:1124 – 8.

5. Howland WJ, Loeffler RK, Starchman DE, Johnson RG. Postirradiation atrophic changes of bone and related complications. Radiology 1975;117: 677 – 85.

6. Jereczek-Fossa BA, Orecchia R. Radiotherapy-induced mandibular bone complications. Cancer Treat Rev 2002;28:65 – 74.

7. Shen ZX, Chen GQ, Ni JH, et al. Use of arsenic trioxide (As2O3) in the treatment of acute promyelocytic leukemia (APL): II. Clinical efficacy and pharmacokinetics in relapsed patients. Blood 1997;89:3354 – 60.

8. Chen GQ, Shi XG, Tang W, et al. Use of arsenic trioxide (As2O3) in the treatment of acute promyelocytic leukemia (APL): I. As2O3 exerts dose-dependent dual effects on APL cells. Blood 1997;89:3345 – 53.

9. Murgo AJ. Clinical trials of arsenic trioxide in hematologic and solid tumors: overview of the National Cancer Institute Cooperative Research and Development Studies. Oncologist 2001;6 Suppl 2:22 – 8.

10. Waxman S, Anderson KC. History of the development of arsenic derivatives in cancer therapy. Oncologist 2001;6 Suppl 2:3 – 10.

11. Roboz GJ, Dias S, Lam G, et al. Arsenic trioxide induces dose- and time-dependent apoptosis of endothelium and may exert an antileukemic effect via inhibition of angiogenesis. Blood 2000;96:1525 – 30.

12. Chen GQ, Zhu J, Shi XG, et al. *In vitro* studies on cellular and molecular mechanisms of arsenic trioxide (As2O3) in the treatment of acute promyelocytic leukemia: As2O3 induces NB4 cell apoptosis with downregulation of Bcl-2 expression and modulation of PML-RAR α/PML proteins. Blood 1996;88:1052 – 61.

13. Chen YC, Lin-Shiau SY, Lin JK. Involvement of reactive oxygen species and caspase 3 activation in arsenite-induced apoptosis. J Cell Physiol 1998;177:324 – 33.

14. Zhu XH, Shen YL, Jing YK, et al. Apoptosis and growth inhibition in malignant lymphocytes after treatment with arsenic trioxide at clinically achievable concentrations. J Natl Cancer Inst 1999;91:772 – 8.

15. Kumar P, Miller AI, Polverini PJ. p38 MAPK mediates γ-irradiation-induced endothelial cell apoptosis, and vascular endothelial growth factor protects endothelial cells through the phosphoinositide 3-kinase-Akt-Bcl-2 pathway. J Biol Chem 2004;279:43352 – 60.

16. Wu J, Haugk K, Plymate SR. Activation of pro-apoptotic p38-MAPK pathway in the prostate cancer cell line M12 expressing a truncated IGF-IR. Horm Metab Res 2003;35:751 – 7.

17. Lowe LC, Senaratne SG, Colston KW. Induction of apoptosis in breast cancer cells by apomine is mediated by caspase and p38 mitogen activated protein kinase activation. Biochem Biophys Res Commun 2005;329:772 – 9.

18. Juretic N, Santibanez JF, Hurtado C, Martinez J. ERK 1,2 and p38 pathways are involved in the proliferative stimuli mediated by urokinase in osteoblastic SaOS-2 cell line. J Cell Biochem 2001;83:92 – 8.

19. Noth U, Tuli R, Seghatoleslami R, et al. Activation of p38 and Smads mediates BMP-2 effects on human trabecular bone-derived osteoblasts. Exp Cell Res 2003;291:201 – 11.

20. Shim MJ, Kim HJ, Yang SJ, et al. Arsenic trioxide induces apoptosis in chronic myelogenous leukemia K562 cells: possible involvement of p38 MAP kinase. J Biochem Mol Biol 2002;35:377 – 83.

21. Verma A, Mohindru M, Deb DK, et al. Activation of Rac1 and the p38 mitogen-activated protein kinase pathway in response to arsenic trioxide. J Biol Chem 2002;277:44988 – 95.

22. Kumar P, Benedict R, Urzua F, et al. Combination treatment significantly enhances the efficacy of antitumor therapy by preferentially targeting angiogenesis. Lab Invest 2005;85:756 – 67.

23. Schneider A, Taboas JM, McCauley LK, Krebsbach PH. Skeletal homeostasis in tissue-engineered bone. J Orthop Res 2003;21:859 – 64.

24. Franceschi RT, Wang D, Krebsbach PH, Rutherford RB. Gene therapy for bone formation: *in vitro* and *in vivo* osteogenic activity of an adenovirus expressing BMP7. J Cell Biochem 2000;78:476 – 86.

25. Krebsbach PH, Kuznetsov SA, Satomura K, et al. Bone formation *in vivo*: comparison of osteogenesis by transplanted mouse and human marrow stromal fibroblasts. Transplantation 1997;63:1059 – 69.

26. Kao YH, Yu CL, Chang LW, Yu HS. Low concentrations of arsenic induce vascular endothelial growth factor and nitric oxide release and stimulate angiogenesis *in vitro*. Chem Res Toxicol 2003;16:460 – 8.

27. Soucy NV, Ihnat MA, Kamat CD, et al. Arsenic stimulates angiogenesis and tumorigenesis *in vivo*. Toxicol Sci 2003;76:271 – 9.

28. Barchowsky A, Roussel RR, Klei LR, et al. Low levels of arsenic trioxide stimulate proliferative signals in primary vascular cells without activating stress effector pathways. Toxicol Appl Pharmacol 1999;159: 65 – 75.

29. Simeonova PP, Wang S, Hulderman T, Luster MI. c-Src-dependent activation of the epidermal growth factor receptor and mitogen-activated protein kinase pathway by arsenic. Role in carcinogenesis. J Biol Chem 2002;277:2945 – 50.

30. Agis H, Weltermann A, Mitterbauer G, et al. Successful treatment with arsenic trioxide of a patient with ATRA-resistant relapse of acute promyelocytic leukemia. Ann Hematol 1999;78:329 – 32.

31. Kumar P, Coltas IK, Kumar B, et al. Bcl-2 protects endothelial cells against γ-radiation via a Raf-MEK-ERK-survivin signaling pathway that is independent of cytochrome c release. Cancer Res 2007;67:1193 – 202.

32. Hayashi T, Hideshima T, Akiyama M, et al. Arsenic trioxide inhibits growth of human multiple myeloma cells in the bone marrow microenvironment. Mol Cancer Ther 2002;1:851 – 60.

33. Lew YS, Brown SL, Griffin RJ, Song CW, Kim JH. Arsenic trioxide causes selective necrosis in solid murine tumors by vascular shutdown. Cancer Res 1999;59:6033 – 7.

34. Griffin RJ, Williams BW, Park HJ, Song CW. Preferential action of arsenic trioxide in solid-tumor microenvironment enhances radiation therapy. Int J Radiat Oncol Biol Phys 2005;61:1516 – 22.

Arsenic trioxide enhances the therapeutic efficacy of radiation treatment of oral squamous carcinoma while protecting bone

Pawan Kumar, Qinghong Gao, Yu Ning, et al.

Mol Cancer Ther 2008;7:2060-2069.